

# Spectroscopic Quantification of the Inverted Singlet–Triplet Gap in Pentaazaphenalene

Kenneth D. Wilson, William H. Styers, Samuel A. Wood, R. Claude Woods, Robert J. McMahon, Zhe Liu, Yang Yang, and Etienne Garand\*



Cite This: *J. Am. Chem. Soc.* 2024, 146, 15688–15692



Read Online

ACCESS |

Metrics & More

Article Recommendations

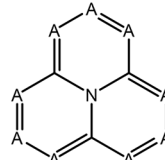
Supporting Information

**ABSTRACT:** We report the direct and accurate spectroscopic quantification of the inverted singlet–triplet gap in 1,3,4,6,9b-pentaazaphenalene. This measurement is achieved by directly probing the lowest singlet and triplet states via high-resolution cryogenic anion photoelectron spectroscopy. The assignment of the first excited singlet state is confirmed by visible absorption spectroscopy in an argon matrix at 20 K. Our measurements yield an inverted singlet–triplet gap with  $\Delta E_{ST} = -0.047(7)$  eV. The accurate quantification of the singlet–triplet gap presented here allows for direct evaluation of various computational electronic structure methods and highlights the critical importance of the proper description of the double excitation character of these electronic states. Overall, this study validates the idea that despite Hund’s multiplicity rule, useful organic chromophores can have inherently inverted singlet–triplet gaps.

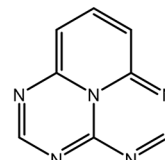
The need to increase fluorescence efficiency in organic light-emitting diodes has led to recent development of chromophores with very small energy difference between the lowest-energy singlet ( $S_1$ ) and triplet ( $T_1$ ) excited states (commonly termed the singlet–triplet gap,  $\Delta E_{ST}$ ).<sup>1–3</sup> In a typical closed-shell organic molecule,  $T_1$  is lower in energy than  $S_1$ , as stated by Hund’s multiplicity rule.<sup>4</sup> Reducing the energy gap between them thus minimizes the loss of excitation energy via the triplet channel by allowing for additional thermally activated delayed fluorescence (TADF) via reverse intersystem crossing, i.e., from  $T_1$  to  $S_1$ . For a simplified two-electron, two-orbital system,  $\Delta E_{ST}$  is proportional to the exchange integral between the two orbitals composing the system.<sup>5</sup> Hund’s multiplicity rule applies in this case because the exchange integral can only be positive. A small  $\Delta E_{ST}$  can be achieved by minimizing the spatial overlap between the HOMO and LUMO, which minimizes the exchange integral.<sup>6</sup> For traditional TADF emitters, this condition is achieved by having spatially separated electron donor and acceptor groups resulting in excitation with significant charge transfer character.<sup>2,3</sup> While the simplified picture is useful for the design of emitters, a more accurate model of  $\Delta E_{ST}$ , which can account for efficient fluorescence and reverse intersystem crossing, must also include contributions from states with local excitation character.<sup>7</sup>

More recently, a different type of chromophore design is being explored in which a minimal exchange integral is achieved by localizing the HOMO and LUMO electron densities on alternating atoms in the molecule.<sup>8–13</sup> The azaphenalenenes, shown in Figure 1, are the most widely studied prototypical molecules exhibiting this characteristic. Intriguingly, many recent computational studies<sup>8,14–22</sup> on azaphenalenenes predict a *negative*  $\Delta E_{ST}$ , i.e., where  $S_1$  is slightly lower in energy than  $T_1$ . The potential for a molecule to break Hund’s multiplicity rule has been known for a long time.<sup>5</sup> Spin

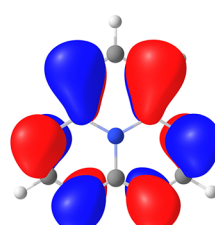
Azaphenalenenes  
A = N or C–H



1,3,4,6,9b-pentaazaphenalene  
(5AP)



5AP HOMO



5AP LUMO

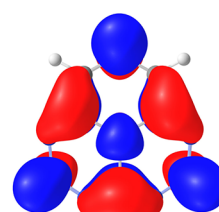


**Figure 1.** Chemical structures of the azaphenalene family and 5AP. HOMO and LUMO depictions of 5AP.

polarization effects<sup>23,24</sup> can overcome a small exchange integral and cause inversion of the two states. In terms of modern electronic structure theory, a negative  $\Delta E_{ST}$  can result from the contribution of doubly excited electronic configurations preferentially stabilizing the  $S_1$  state over the  $T_1$  state.<sup>25</sup>

Received: April 12, 2024

Revised: May 23, 2024

Accepted: May 24, 2024

Published: May 30, 2024



ACS Publications

© 2024 American Chemical Society

15688

<https://doi.org/10.1021/jacs.4c05043>  
*J. Am. Chem. Soc.* 2024, 146, 15688–15692

Indeed, many theoretical studies have shown that the inclusion of doubly excited configurations is crucial in predicting a negative  $\Delta E_{ST}$  in azaphenalenenes.<sup>8,18–20</sup> However, the calculated  $\Delta E_{ST}$  values are small and well within the typical uncertainties<sup>26</sup> expected for most excited-state computational methods accessible for molecules of the size of azaphenalenenes. Accurate predictions of the magnitude and possible inversion of  $\Delta E_{ST}$  in azaphenalenenes are still at the forefront of the electronic structure theory. It remains uncertain whether singlet–triplet inversion is generally possible in azaphenalenenes or if it is simply an artifact of the approximate electronic structure theory used.<sup>27</sup>

One crucial, but still missing, piece of information is the accurate spectroscopic quantification of  $\Delta E_{ST}$  in these chromophores, which is difficult to obtain because of the spin-forbidden nature of the  $S_0$ – $T_1$  transition and the difficulties arising from the near degeneracy of  $S_1$  and  $T_1$ . Instead, chromophores with a small  $\Delta E_{ST}$  are usually characterized via the temperature dependence of the delayed fluorescence rate and quenching of the delayed fluorescence signal by  $O_2$ . Such experimental approaches have shown the presence of an inverted singlet–triplet gap in a handful of functionalized azaphenalenenes.<sup>9,11,12,28,29</sup>

Here we use cryogenic high-resolution anion photoelectron (PE) spectroscopy<sup>30,31</sup> to provide a direct spectroscopic quantification of the inverted singlet–triplet gap in 1,3,4,6,9b-pentaazaphenalene (**SAP**), whose structure is shown in Figure 1. **SAP** is easily accessible via a single-step synthesis from commercially available reagents<sup>32</sup> and has been predicted to offer a good trade-off between having a negative  $\Delta E_{ST}$  and maximizing the fluorescence rate for potential light emission applications.<sup>14</sup> In anion PE spectroscopy, electrons are photodetached from a molecular anion such as the **SAP**<sup>–</sup> radical anion, and their kinetic energies (eKE) are measured to map the vibronic energy levels of the corresponding neutral molecule. Starting from the radical anion ground-state ( $D_0$ ), the photodetachment selection rules permit the spectroscopic observation of both neutral singlet and triplet states and therefore provide direct spectroscopic quantification of  $\Delta E_{ST}$ . Moreover, the chromophores are probed at low temperature and without solvent perturbation, yielding experimental excitation energies that can be directly compared with the results of electronic structure computations. This experimental approach has been successfully used to quantify  $\Delta E_{ST}$  in a variety of organic chromophores, such as the very small singlet–triplet gap in azulene.<sup>33</sup>

The anion PE spectra shown in the bottom panel of Figure 2 were acquired using our high-resolution cryogenic anion photoelectron spectrometer, described previously,<sup>34</sup> and in the Supporting Information. These spectra are plotted as a function of electron binding energy (eBE), which is defined as the difference between the photodetachment photon energy and measured eKE.

The first group of peaks, located in the 1.20–1.45 eV eBE range, is assigned to transitions to the neutral **SAP** ground electronic state ( $S_0$ ). Peak A is assigned to the 0–0 origin transition, and its position yields an adiabatic electron affinity of 1.235(2) eV for **SAP**. This assignment is in good agreement with the calculated value of 1.20 eV at the B3LYP-D3/ma-def2-TZVPP level of theory. The weaker features in this group are assigned to  $D_0$ – $S_0$  vibronic transitions, in agreement with the Franck–Condon simulations shown in the Supporting Information. The second group of peaks appears in the 3.15–

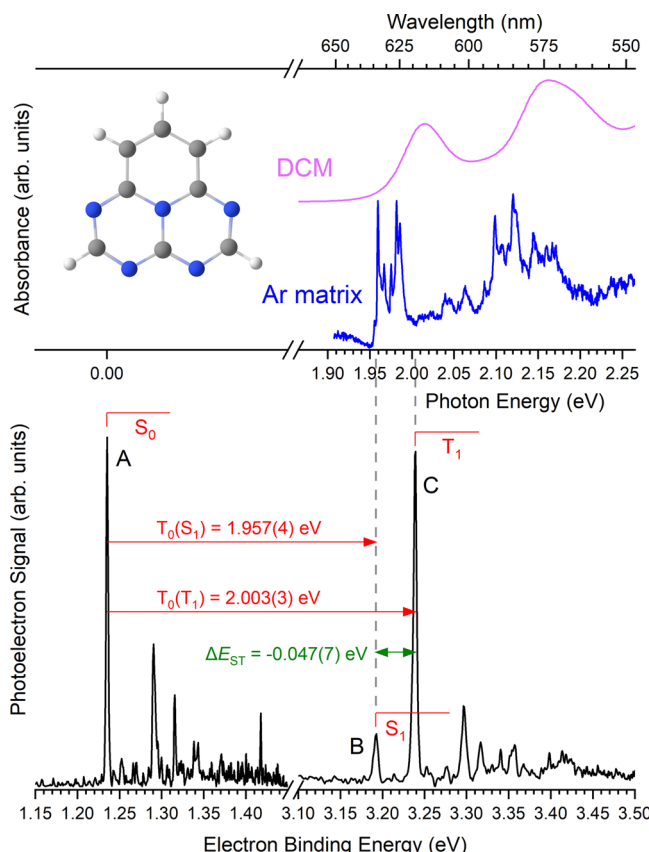


**Figure 2.** (top panel) Absorption spectra of **SAP** in DCM and in annealed 20 K argon matrix. (bottom panel) Anion photoelectron spectra of **SAP**<sup>–</sup> in the energy ranges corresponding to the neutral  $S_0$ ,  $S_1$ , and  $T_1$  states. The horizontal scales of both panels are aligned to allow for a direct comparison of the position of the  $S_1$  state in the absorption and photoelectron spectra.

3.45 eV eBE range, where  $T_1$  and  $S_1$  are expected. Based on computed Franck–Condon spectra, we expect the 0–0 origin transition to be the most intense feature for both the  $S_1$  and  $T_1$  state. Therefore, we assign the predominant feature, peak C at eBE = 3.239(3) eV, to be one of the origin transitions. The weaker peak B, at eBE = 3.192(4) eV, is the only feature located at lower eBE than peak C. In the absence of hot bands, which is reasonably expected for anions thermalized to  $\sim$ 10 K, peak B can only be assigned as the origin transition of the other electronic state. Subtracting the electron affinity determined above thus yields adiabatic term energies of 1.957(4) and 2.003(3) eV for these two states relative to the  $S_0$  state. Unfortunately, the PE spectra themselves do not allow us to unambiguously distinguish which transition corresponds to  $S_1$  vs  $T_1$ .

To achieve an unambiguous assignment, we turn to electronic absorption spectroscopy where only the  $S_0$ – $S_1$  transition is spin-allowed. The absorption spectrum of **SAP** in dichloromethane (DCM) solution is shown in the top panel of Figure 2 (purple trace). To facilitate a direct comparison with the anion PE spectra, the absorption spectrum is plotted in terms of photon energy (eV) with the origin of the energy axis aligned with the  $S_0$  origin transition (peak A). The more familiar wavelength (nm) units are shown on the top axis. The  $S_0$ – $S_1$  transition is a broad feature centered at around 2.02 eV, which is slightly blue-shifted with respect to both peaks B and C. Solvents with higher polarity induce a larger solvatochromic

**Table 1.** Summary of Computed Transitions Energies and  $\Delta E_{ST}$  for SAP

computational method	$E(S_0-S_1)$ (eV)	$E(S_0-T_1)$ (eV)	$\Delta E_{ST}$ (eV)	ref
<b>vertical transition energies</b>				
ADC(2)/def2-TZVP	2.154	2.296	-0.142	18
ADC(2)/aug-cc-pVTZ	2.159	2.298	-0.139	21
CC2/def2-TZVP	2.231	2.365	-0.134	18
CC2/aug-cc-pVTZ	2.235	2.366	-0.131	21
CC3/aug-cc-pVDZ	2.164	2.284	-0.120	21
EOM-CCSD/cc-pVDZ	2.251	2.329	-0.078	14
EOM-CCSD/cc-pVTZ	2.343	2.372	-0.030	this work
EOM-CCSD/aug-cc-pVTZ	2.374	2.394	-0.020	21
EOM-CCSDt/cc-pVTZ	2.223	2.315	-0.092	this work
<b>(0–0) transition energies</b>				
ADC(2)/def2-TZVP	1.901	1.995	-0.094	18
CC2/def2-TZVP	1.971	2.056	-0.085	18
EOM-CCSD/cc-pVTZ//B3LYP	2.192	2.168	+0.024	this work
EOM-CCSDt/cc-pVTZ//B3LYP	1.942	1.964	-0.022	this work
experimental	1.957(4)	2.003(3)	-0.047(7)	this work

blue-shift in SAP (see Figure S4). This result is consistent with predictions from DFT computations with a polarizable continuum model (Table S2). However, because the magnitude of the solvatochromic blue-shift is difficult to compute accurately, the solution phase absorption spectrum alone is still insufficient. Hence, we acquired the absorption spectrum of SAP in an annealed 20 K argon matrix, as shown also in Figure 2A (blue trace). Similar to other solvents, argon is expected to produce a solvatochromic blue-shift, but with a much smaller magnitude than DCM. The  $S_0-S_1$  origin transition in the Ar matrix appears as several peaks in the 1.95–2.00 eV range which we attribute to a distribution of unique matrix sites based on comparison of annealed and unannealed matrix spectra (see the Supporting Information). Nonetheless, these features are all located above peak B and below peak C. Therefore, we can now conclusively assign peak B in the PE spectrum to the 0–0 origin transition of the  $S_1$  state, which leaves peak C as the 0–0 origin transition of the  $T_1$  state. This combination of anion PE spectroscopy and electronic absorption spectroscopy thus provides direct evidence of an inverted singlet–triplet gap in SAP. The eBE difference between peaks B and C yields a value of -0.047(7) eV for the singlet–triplet gap.

Our quantitative experimental measurement of  $\Delta E_{ST}$  for an unsubstituted azaphenalene provides an important benchmark for various electronic structure methods. Table 1 shows a summary of some of the most important computational results for SAP. We note that most computations in Table 1 use the difference between the vertical excitation energies of  $S_1$  and  $T_1$  to calculate  $\Delta E_{ST}$ . This approximation avoids performing expensive computations by assuming that the molecular geometry and vibrational frequencies of the  $S_1$  and  $T_1$  states are very similar to each other. With this approach and using the ADC(2), CC2, and CC3 wave function methods, Tuckova et al.<sup>18</sup> and Loos et al.<sup>21</sup> reported  $\Delta E_{ST}$  which are ~0.07–0.09 eV more negative than the experimental value. The closest values are obtained with the EOM-CCSD method. In particular, the use of EOM-CCSD with larger triple- $\zeta$  basis sets yields  $\Delta E_{ST}$  values in excellent agreement with the experimental value (-0.047 eV).

While most of these computational methods yield reasonable  $\Delta E_{ST}$  values, they notably exhibit sharper differences in the computed vertical transition energies (see Table

1). Unfortunately, the accuracy of these values cannot be directly verified because they do not correspond to any spectroscopic observables in polyatomic molecules due to the geometry relaxation being distributed over a large number of normal modes. Fortunately, Tuckova et al.<sup>18</sup> did report the adiabatic and zero-point energy (ZPE) corrections to the transition energies at the ADC(2) and CC2 level of theory. These corrections result in  $\Delta E_{ST}$  values that are slightly less negative compared to those obtained with vertical transition energies and in better agreement with the experimental values. Very importantly, the computed  $S_1$  and  $T_1$  (0–0) transitions are within ~0.05 eV of the experimental measurements. This indicates that the good  $\Delta E_{ST}$  agreement for these methods is not a fortuitous cancellation of errors involved in subtracting the vertical  $S_1$  and  $T_1$  transition energies.

However, the application of adiabatic and ZPE corrections to the EOM-CCSD vertical transitions leads to a slightly positive  $\Delta E_{ST}$ . For example, our computations using the B3LYP geometries and frequencies with EOM-CCSD/cc-pVTZ excitation energies yield a  $\Delta E_{ST}$  of +0.024 eV, in disagreement with the experimental observation of an inverted singlet–triplet in SAP. Moreover, the EOM-CCSD computed 0–0 transitions energies are ~0.17–0.25 eV higher than the experimental values. This is a very important result because this method is generally considered to be very accurate and often used as the benchmark for more approximate approaches. The observed discrepancy probably originates from the known issues of EOM-CCSD in accurately describing states with significant double excitation character.<sup>35–38</sup> To verify this hypothesis, we performed equation of motion coupled cluster with single, double, and active triples (EOM-CCSDt/cc-pVTZ) calculations, in which the triply excited clusters are computed in a small active space comprising 3 occupied and 3 virtual orbitals.<sup>39</sup> This approach yields an inverted singlet–triplet gap with an  $\Delta E_{ST}$  of -0.022 eV, in much better agreement with the experimental value. The computed 0–0 transitions energies are also within ~0.02–0.04 eV of the experimental values. This agreement highlights the critical importance of properly describing the double excitation character of these states to accurately predict singlet–triplet gap inversion.

In conclusion, by mapping both  $S_1$  and  $T_1$  states via anion PE spectroscopy and confirming the position of the  $S_1$  state by

electronic absorption spectroscopy, we obtained a direct and accurate spectroscopic measurement of the inverted singlet–triplet gap in **SAP**. Our results validate the idea that despite Hund’s multiplicity rule, certain useful organic chromophores can have an inherently inverted singlet–triplet gap. The accurate experimental quantification of  $\Delta E_{\text{ST}}$  in **SAP** presented here also allows for the validation of computational electronic structure methods that may be useful in aiding the search and design of such chromophores. In terms of useful applications in the field of light-emitting diodes, the main disadvantage of the azaphenalenone cores lies in having a generally weak  $S_0$ – $S_1$  oscillator strength, which can limit the fluorescence yield. However, Pollice et al.<sup>14</sup> have shown that the oscillator strength can be significantly improved by selecting proper ring substituents. Such functionalization of the azaphenalenone core is expected to influence the chromophore’s HOMO and LUMO via electron delocalization and electron donating/withdrawing effects. Therefore, experimental quantification and validation of the theoretical modeling of the substituent effects on  $\Delta E_{\text{ST}}$  are certainly warranted.

## ■ ASSOCIATED CONTENT

### SI Supporting Information

The Supporting Information is available free of charge at <https://pubs.acs.org/doi/10.1021/jacs.4c05043>.

Details of the **SAP** synthesis, experimental and computational methods, solvatochromic shift computations, Franck–Condon simulations, and matrix annealing experiments (PDF)

## ■ AUTHOR INFORMATION

### Corresponding Author

Etienne Garand – Department of Chemistry, University of Wisconsin—Madison, Madison, Wisconsin 53706, United States;  [orcid.org/0000-0001-5062-5453](https://orcid.org/0000-0001-5062-5453); Email: [egarand@wisc.edu](mailto:egarand@wisc.edu)

### Authors

Kenneth D. Wilson – Department of Chemistry, University of Wisconsin—Madison, Madison, Wisconsin 53706, United States

William H. Styers – Department of Chemistry, University of Wisconsin—Madison, Madison, Wisconsin 53706, United States

Samuel A. Wood – Department of Chemistry, University of Wisconsin—Madison, Madison, Wisconsin 53706, United States

R. Claude Woods – Department of Chemistry, University of Wisconsin—Madison, Madison, Wisconsin 53706, United States;  [orcid.org/0000-0003-0865-4693](https://orcid.org/0000-0003-0865-4693)

Robert J. McMahon – Department of Chemistry, University of Wisconsin—Madison, Madison, Wisconsin 53706, United States;  [orcid.org/0000-0003-1377-5107](https://orcid.org/0000-0003-1377-5107)

Zhe Liu – Department of Chemistry, University of Wisconsin—Madison, Madison, Wisconsin 53706, United States

Yang Yang – Department of Chemistry, University of Wisconsin—Madison, Madison, Wisconsin 53706, United States;  [orcid.org/0000-0001-8572-5155](https://orcid.org/0000-0001-8572-5155)

Complete contact information is available at: <https://pubs.acs.org/doi/10.1021/jacs.4c05043>

## Funding

This work was supported by the National Science Foundation under grants CHE-2349257 (to E.G., for the anion photo-electron work), CHE-2245738, (to R.J.M., for the matrix absorption work), and CHE-2238473 (to Y.Y., for the computational work). Computations used resources from the UW-Madison Center for High Throughput Computing.<sup>40</sup>

## Notes

The authors declare no competing financial interest.

## ■ REFERENCES

- (1) Uoyama, H.; Goushi, K.; Shizu, K.; Nomura, H.; Adachi, C. Highly Efficient Organic Light-Emitting Diodes from Delayed Fluorescence. *Nature* **2012**, *492* (7428), 234–238.
- (2) Liang, X.; Tu, Z.-L.; Zheng, Y.-X. Thermally Activated Delayed Fluorescence Materials: Towards Realization of High Efficiency through Strategic Small Molecular Design. *Chem. – Eur. J.* **2019**, *25* (22), 5623–5642.
- (3) Penfold, T. J.; Dias, F. B.; Monkman, A. P. The Theory of Thermally Activated Delayed Fluorescence for Organic Light Emitting Diodes. *Chem. Commun.* **2018**, *54* (32), 3926–3935.
- (4) Hund, F. Zur Deutung Verwickelter Spektren, Insbesondere Der Elemente Scandium Bis Nickel. *Z. Für Phys.* **1925**, *33* (1), 345–371.
- (5) Slater, J. The Theory of Complex Spectra. *Phys. Rev.* **1929**, *34* (10), 1293–1322.
- (6) Chen, T.; Zheng, L.; Yuan, J.; An, Z.; Chen, R.; Tao, Y.; Li, H.; Xie, X.; Huang, W. Understanding the Control of Singlet-Triplet Splitting for Organic Exciton Manipulating: A Combined Theoretical and Experimental Approach. *Sci. Rep.* **2015**, *5*, 10923.
- (7) de Silva, P.; Kim, C.; Zhu, T.; Van Voorhis, T. Extracting Design Principles for Efficient Thermally Activated Delayed Fluorescence (TADF) from a Simple Four-State Model. *Chem. Mater.* **2019**, *31* (17), 6995–7006.
- (8) de Silva, P. Inverted Singlet-Triplet Gaps and Their Relevance to Thermally Activated Delayed Fluorescence. *J. Phys. Chem. Lett.* **2019**, *10* (18), 5674–5679.
- (9) Li, J.; Nomura, H.; Miyazaki, H.; Adachi, C. Highly Efficient Exciplex Organic Light-Emitting Diodes Incorporating a Heptazine Derivative as an Electron Acceptor. *Chem. Commun.* **2014**, *50* (46), 6174–6176.
- (10) Li, J.; Zhang, Q.; Nomura, H.; Miyazaki, H.; Adachi, C. Thermally Activated Delayed Fluorescence from  $^3n\pi^*$  to  $^1n\pi^*$  Up-Conversion and Its Application to Organic Light-Emitting Diodes. *Appl. Phys. Lett.* **2014**, *105* (1), 013301.
- (11) Li, J.; Nakagawa, T.; MacDonald, J.; Zhang, Q.; Nomura, H.; Miyazaki, H.; Adachi, C. Highly Efficient Organic Light-Emitting Diode Based on a Hidden Thermally Activated Delayed Fluorescence Channel in a Heptazine Derivative. *Adv. Mater.* **2013**, *25* (24), 3319–3323.
- (12) Aizawa, N.; Pu, Y.; Harabuchi, Y.; Nihonyanagi, A.; Ibuka, R.; Inuzuka, H.; Dhara, B.; Koyama, Y.; Nakayama, K.; Maeda, S.; Araoka, F.; Miyajima, D. Delayed Fluorescence from Inverted Singlet and Triplet Excited States. *Nature* **2022**, *609* (7927), 502.
- (13) Hatakeyama, T.; Shireen, K.; Nakajima, K.; Nomura, S.; Nakatsuka, S.; Kinoshita, K.; Ni, J.; Ono, Y.; Ikuta, T. Ultrapure Blue Thermally Activated Delayed Fluorescence Molecules: Efficient HOMO–LUMO Separation by the Multiple Resonance Effect. *Adv. Mater.* **2016**, *28* (14), 2777–2781.
- (14) Pollice, R.; Friederich, P.; Lavigne, C.; Gomes, G.; Aspuru-Guzik, A. Organic Molecules with Inverted Gaps between First Excited Singlet and Triplet States and Appreciable Fluorescence Rates. *MATTER* **2021**, *4* (5), 1654–1682.
- (15) Sanz-Rodrigo, J.; Ricci, G.; Olivier, Y.; Sancho-Garcia, J. Negative Singlet-Triplet Excitation Energy Gap in Triangle-Shaped Molecular Emitters for Efficient Triplet Harvesting. *J. Phys. Chem. A* **2021**, *125* (2), 513–522.
- (16) Pios, S.; Huang, X.; Sobolewski, A.; Domcke, W. Triangular Boron Carbon Nitrides: An Unexplored Family of Chromophores

with Unique Properties for Photocatalysis and Optoelectronics. *Phys. Chem. Chem. Phys.* **2021**, *23* (23), 12968–12975.

(17) Sobolewski, A.; Domcke, W. Are Heptazine-Based Organic Light-Emitting Diode Chromophores Thermally Activated Delayed Fluorescence or Inverted Singlet-Triplet Systems? *J. Phys. Chem. Lett.* **2021**, *12* (29), 6852–6860.

(18) Tuckova, L.; Straka, M.; Valiev, R.; Sundholm, D. On the Origin of the Inverted Singlet-Triplet Gap of the 5th Generation Light-Emitting Molecules. *Phys. Chem. Chem. Phys.* **2022**, *24* (31), 18713–18721.

(19) Alipour, M.; Izadkhast, T. Do Any Types of Double-Hybrid Models Render the Correct Order of Excited State Energies in Inverted Singlet-Triplet Emitters? *J. Chem. Phys.* **2022**, *156* (6), 064302.

(20) Sancho-Garcia, J.; Bremond, E.; Ricci, G.; Perez-Jimenez, A.; Olivier, Y.; Adamo, C. Violation of Hund's Rule in Molecules: Predicting the Excited-State Energy Inversion by TD-DFT with Double-Hybrid Methods. *J. Chem. Phys.* **2022**, *156* (3), 034105.

(21) Loos, P.-F.; Lippurini, F.; Jacquemin, D. Heptazine, Cyclazine, and Related Compounds: Chemically-Accurate Estimates of the Inverted Singlet-Triplet Gap. *J. Phys. Chem. Lett.* **2023**, *14* (49), 11069–11075.

(22) Garner, M. H.; Blaskovits, J. T.; Corminboeuf, C. Enhanced Inverted Singlet-Triplet Gaps in Azaphenalenes and Non-Alternant Hydrocarbons. *Chem. Commun.* **2024**, *60* (15), 2070–2073.

(23) Koseki, S.; Nakajima, T.; Toyota, A. Violation of Hund Multiplicity Rule in the Electronically Excited-States of Conjugated Hydrocarbons. *Can. J. Chem.-Rev. Can. Chim.* **1985**, *63* (7), 1572–1579.

(24) Kollmar, H.; Staemmler, V. Violation of Hund's Rule by Spin Polarization in Molecules. *Theor. Chim. Acta* **1978**, *48* (3), 223–239.

(25) Morgan, J.; Kutzelnigg, W. Hund Rules, the Alternating Rule, and Symmetry Holes. *J. Phys. Chem.* **1993**, *97* (10), 2425–2434.

(26) Winter, N.; Graf, N.; Leutwyler, S.; Hattig, C. Benchmarks for 0–0 Transitions of Aromatic Organic Molecules: DFT/B3LYP, ADC(2), CC2, SOS-CC2 and SCS-CC2 Compared to High-Resolution Gas-Phase Data. *Phys. Chem. Chem. Phys.* **2013**, *15* (18), 6623–6630.

(27) Dreuw, A.; Hoffmann, M. The Inverted Singlet-Triplet Gap: A Vanishing Myth? *Front. Chem.* **2023**, DOI: [10.3389/fchem.2023.1239604](https://doi.org/10.3389/fchem.2023.1239604).

(28) Li, J.; Li, Z.; Liu, H.; Gong, H.; Zhang, J.; Li, X.; Wang, Y.; Guo, Q. Down-Conversion-Induced Delayed Fluorescence via an Inverted Singlet-Triplet Channel. *DYES PIGMENTS* **2022**, *203*, 110366.

(29) Ehrmaier, J.; Rabe, E.; Pristash, S.; Corp, K.; Schlenker, C.; Sobolewski, A.; Domcke, W. Singlet-Triplet Inversion in Heptazine and in Polymeric Carbon Nitrides. *J. Phys. Chem. A* **2019**, *123* (38), 8099–8108.

(30) Leon, I.; Yang, Z.; Liu, H.; Wang, L. The Design and Construction of a High-Resolution Velocity-Map Imaging Apparatus for Photoelectron Spectroscopy Studies of Size-Selected Clusters. *Rev. Sci. Instrum.* **2014**, *85* (8), 083106.

(31) Hock, C.; Kim, J.; Weichman, M.; Yacovitch, T.; Neumark, D. Slow Photoelectron Velocity-Map Imaging Spectroscopy of Cold Negative Ions. *J. Chem. Phys.* **2012**, *137* (24), 244201.

(32) Shaw, J. T.; O'Connor, M. E.; Allen, R. C.; Westler, W. M.; Stefanko, B.D. Fused S-Triazino Heterocycles. II. 1,3,4,6,9b-Pentaazaphenalenes and 1,3,4,6,7,9b-Hexaazaphenalene. *J. Heterocycl. Chem.* **1974**, *11* (4), 627–630.

(33) Vosskotter, S.; Konieczny, P.; Marian, C.; Weinkauf, R. Towards an Understanding of the Singlet-Triplet Splittings in Conjugated Hydrocarbons: Azulene Investigated by Anion Photoelectron Spectroscopy and Theoretical Calculations. *Phys. Chem. Chem. Phys.* **2015**, *17* (36), 23573–23581.

(34) Kregel, S. J.; Thurston, G. K.; Zhou, J.; Garand, E. A Multi-Plate Velocity-Map Imaging Design for High-Resolution Photoelectron Spectroscopy. *J. Chem. Phys.* **2017**, *147* (9), No. 094201.

(35) Izsák, R. Single-Reference Coupled Cluster Methods for Computing Excitation Energies in Large Molecules: The Efficiency and Accuracy of Approximations. *WIREs Comput. Mol. Sci.* **2020**, *10* (3), No. e1445.

(36) Schreiber, M.; Silva-Junior, M. R.; Sauer, S. P. A.; Thiel, W. Benchmarks for Electronically Excited States: CASPT2, CC2, CCSD, and CC3. *J. Chem. Phys.* **2008**, *128* (13), No. 134110.

(37) Watts, J. D.; Bartlett, R. J. The Inclusion of Connected Triple Excitations in the Equation-of-motion Coupled-cluster Method. *J. Chem. Phys.* **1994**, *101* (4), 3073–3078.

(38) Watts, J. D.; Bartlett, R. J. Economical Triple Excitation Equation-of-Motion Coupled-Cluster Methods for Excitation Energies. *Chem. Phys. Lett.* **1995**, *233* (1), 81–87.

(39) Kowalski, K.; Piecuch, P. The Active-Space Equation-of-Motion Coupled-Cluster Methods for Excited Electronic States: The EOMCCSDt Approach. *J. Chem. Phys.* **2000**, *113* (19), 8490–8502.

(40) Center for High Throughput Computing, 2006. DOI: [10.21231/GNT1-HW21](https://doi.org/10.21231/GNT1-HW21).